Accepted Manuscript

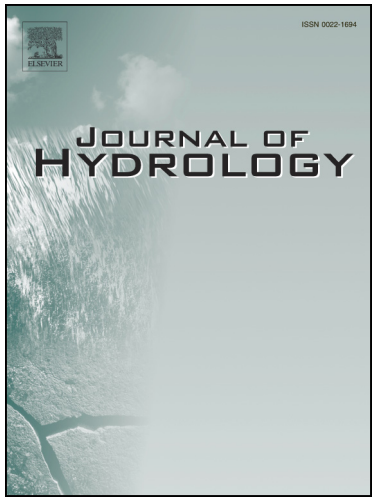

Research papers

Spatiotemporal geostatistical modeling of groundwater levels under a Bayesian framework using means of physical background

Emmanouil A. Varouchakis, Panagiota G. Theodoridou, George P. Karatzas

PII: S0022-1694(19)30500-1
DOI: https://doi.org/10.1016/j.jhydrol.2019.05.055
Reference: HYDROL 23788

To appear in: *Journal of Hydrology*

Received Date: 22 November 2018
Revised Date: 16 May 2019
Accepted Date: 17 May 2019

Please cite this article as: Varouchakis, E.A., Theodoridou, P.G., Karatzas, G.P., Spatiotemporal geostatistical modeling of groundwater levels under a Bayesian framework using means of physical background, *Journal of Hydrology* (2019), doi: https://doi.org/10.1016/j.jhydrol.2019.05.055

This is a PDF file of an unedited manuscript that has been accepted for publication. As a service to our customers we are providing this early version of the manuscript. The manuscript will undergo copyediting, typesetting, and review of the resulting proof before it is published in its final form. Please note that during the production process errors may be discovered which could affect the content, and all legal disclaimers that apply to the journal pertain.

ACCEPTED MANUSCRIPT

Spatiotemporal geostatistical modeling of groundwater levels under a Bayesian framework using means of physical background

Emmanouil A. Varouchakis*, Panagiota G. Theodoridou, George P. Karatzas

School of Environmental Engineering, Technical University of Crete, Chania, Greece

*Corresponding author: e-mail: varuhaki@mred.tuc.gr, tel : +302821037803

Abstract

The joint spatiotemporal modeling of aquifer level fluctuations provides a significant tool in the prediction of groundwater levels at unvisited locations. Two types of variogram functions, appropriately modified to incorporate physical information, are presented and compared under Space-time Residual kriging methodology using the Bayesian Bootstrap idea to quantify uncertainty. The spatiotemporal trend is approximated using a component of physical meaning. A recently developed Spartan type non-separable variogram function employs tools of physical meaning to enhance the efficiency and reliability of spatiotemporal geostatistical modeling in groundwater applications. In addition, the product-sum space-time variogram is applied and involves in the separable variogram functions a scale factor of hydraulic conductivity directional ratio. The proposed variogram functions involve a non-Euclidean distance metric and are mathematically valid (i.e., constitutes permissible models). Herein, the efficiency of the proposed tools is tested using groundwater level data from an alluvial unconfined aquifer. Both functions provide improved results compared to those of the Space-time Ordinary kriging. Between the two, the non-separable one has the most efficient performance.

ACCEPTED MANUSCRIPT

Keywords

non-separable variogram; space-time kriging; groundwater; Manhattan distance; Bayesian Bootstrap idea; non-Euclidean distance

1.0 Introduction

Spatiotemporal geostatistics is a significant tool for groundwater level modeling and resources management. A common field where geostatistics is applied is the one of hydrology, e.g. to model the spatial/temporal variability of aquifer level as a random field. Successful groundwater flow modelling, using physically based models and numerical techniques, requires detailed information on the spatial variation of the aquifer variables, input and boundary conditions. On the other hand, statistical stochastic approaches like geostatistics are suitable to determine the groundwater level space-time variations at scarce and sparse monitored areas (Kitanidis, 1997).

Estimation of groundwater levels at grid points using measurements at random points is necessary to apply groundwater simulation models. In most geohydrological studies the initial data are in the form of scattered data. A basic task is to use these values in order to provide the spatial variability of the variable under study (Rouhani, 1986). Kriging and other forms of regularization can be useful in many circumstances in developing ground water models, map water table (which is basic for regional hydrogeological investigations), identification of groundwater flow direction and zones of recharge or discharge (Desbarats et al., 2002; Hill, 2006; Varouchakis and Hristopulos, 2013). Groundwater flow models often needs to be defined using limited data or after extensive calibration uncertainties still exist. On the other hand, kriging techniques does not guarantee consistency with the physics of groundwater flow, but can reliably represent the hydraulic head fields (Rivest et al., 2008). Due to scarcity of information about the hydrogeological system, boundary conditions and hydrogeological detailed data or gaps in groundwater level spatial and temporal measurements, geostatistical models in spatial or spatiotemporal context are extensively applied to represent the

ACCEPTED MANUSCRIPT

hydraulic head field variations e.g. (Baú and Mayer, 2006; Bierkens et al., 2001; Kumar, 2007; Lyon et al., 2006; Razavi et al., 2012; Ruybal et al., 2019; Theodossiou and Latinopoulos, 2006; Tonkin and Larson, 2002; Varouchakis and Hristopulos, 2017). There are also works regarding groundwater levels or groundwater contamination where the results of kriging techniques were successfully compared with the results of numerical models and apply as surrogates (An et al., 2015; Asher et al., 2015; Baú and Mayer, 2006; Ma et al., 1999; Pardo-Igúzquiza and Chica-Olmo, 2004; Zhao et al., 2016).

Generally, geostatistical modelling can aid a physically based modelling approach e.g, providing the initial conditions of groundwater level distribution or to provide a reliable representation of groundwater levels space-time variations based on available data. The implementation of geostatistical methods is based on the calculation of data spatial and/or temporal dependence.

The geostatistical analysis of space-time dependent data has initially been performed applying separable covariance functions involving the combination of discrete spatial and temporal variogram models (Cressie, 1993; Dimitrakopoulos and Luo, 1994; Rodriguez-Iturbe and Mejia, 1974; Rouhani and Myers, 1990). On the other hand, the non-separable covariance functions, developed the last two decades, often include components with physical meaning. Dynamic rules or differential equations employed in these functions help to improve prediction accuracy (Christakos, 2000; Christakos and Hristopulos, 1998; Gneiting, 2002; Kolovos et al., 2004; Porcu et al., 2006).

Up to now, spatiotemporal covariance functions for groundwater level applications have not been established. However, spatiotemporal covariance functions based on physical ground have been developed and are mostly applied in atmospheric pollution and synthetic data. Such research has been presented in the past, i.e. the Cressie-Huang functions (Cressie and Huang, 1999), Gneiting's non separable models (Gneiting, 2002), a series of non-separable models based on physical laws and dynamic rules in (Kolovos et al., 2004) and the non-separable functions that replace the covariance with a spectral density function (Porcu et al., 2008).

ACCEPTED MANUSCRIPT

Previous research on geostatistical analysis of scarce groundwater level datasets has shown that the approximation of a spatial trend using secondary information (e.g., topographic and geomorphologic features), improves the predictions of groundwater level e.g. (Desbarats et al., 2002; Varouchakis and Hristopulos, 2013). Therefore, the introduction of a spatiotemporal trend model for space-time geostatistical analysis of groundwater level would be an interesting approach to improve spatiotemporal predictions. The incorporation of temporal trend, in terms of an exponentially weighted moving average filter, and the spatial trend in terms of a groundwater flow equation resulted in the spatiotemporal trend applied in the present work.

The estimated trend and the residual component are combined in terms of space-time Residual Kriging (STRK) methodology, while the investigation of the spatiotemporal trend variance is also important due to its complexity. To estimate the variance associated with the trend, three components were considered: the predictors at the prediction point, the variance of the temporal trend function and the variance resulted from the groundwater flow equation. The variance terms are necessary to be determined for the accurate STRK estimations and the overall variance calculation. For this reason, a Bayesian kriging type under the Bootstrap idea called Empirical Bayesian Kriging (Pilz and Spöck, 2008) was applied to capture the range of the spatiotemporal model uncertainty in terms of the parameters involved and the estimated covariance function.

Given a time series at specific spatial points and considering the time as an extra dimension, the spatiotemporal geostatistical analysis aims to model multiple time series of data performing interpolation and prediction. The interpolation accuracy is tested using leave one out cross validation, while predictions assessment applies validating measurements on the examined temporal scale (i.e. wet and dry periods of a hydrological year) in a time-forward mode. The latter means that the spatiotemporal process prediction occur time-forward according to the determined properties that are defined by the space-time variogram.

ACCEPTED MANUSCRIPT

Space–time kriging can be applied for interpolation purposes (Heuvelink and Griffith, 2010; Júnez-Ferreira and Herrera, 2013; Ruybal et al., 2019; Snepvangers et al., 2003) but also in the form of time–forward kriging using proximities such as the variogram or covariance parameters i.e. correlation length to forecast the spatio–temporal process (Christakos, 2000). Measurements usually are regularly taken on the time domain compared to the spatial domain, hence estimation is most often in time extrapolation mode (Kyriakidis and Journel, 1999). Space-time kriging is one of those methodologies that can be applied for extrapolation-prediction (Gneiting et al., 2007; Kyriakidis and Journel, 1999; Rouhani and Myers, 1990). Extrapolation-prediction assumes that the calculated variogram properties applies outside the space-time range of data. Specifically, consider a purely spatial random field with stationary covariance function and suppose that the entire field moves time-forward. The resulting spatio-temporal random field has stationary covariance with correlation lengths that indicates the spatial and temporal correlation distance of the measurements and therefore the reliable prediction time window (Gneiting et al., 2007).

Many works have applied successfully Space-time kriging for prediction (time-forward prediction) purposes at different spatial locations of variable datasets e.g groundwater level (Ruybal et al., 2019; Varouchakis and Hristopulos, 2017), carbon dioxide using satellite data (Tadić et al., 2017; Zeng et al., 2014), irradiance (Aryaputera et al., 2015; Yang et al., 2013), power load (Chaojun et al., 2014), municipal water demand (Lee et al., 2010), and temperatures (Hengl et al., 2011)

A random field $Z(\mathbf{s},t)$ is used to represent the spatiotemporal stochastic process at *N* space-time coordinates $(\mathbf{s}_i,t_i),\ldots,(\mathbf{s}_N,t_N)$, (Cressie and Huang, 1999; Giraldo Henao, 2009) where the variable under study is monitored. The spatiotemporal random field (S/TRF) $Z(\mathbf{s},t)$ is divided to a mean factor $m_Z(\mathbf{s},t)$ modeling the presence of a correlated trend and a residual S/TRF factor $Z'(s,t)$ modeling space-time variations around that trend (Christakos, 1991; Kyriakidis and Journel, 1999). The first goal of this work was the development of a reliable geostatistical model to represent the space-time variations of groundwater levels at the study aquifer. The second goal of

ACCEPTED MANUSCRIPT

this study was to employ novel covariance functions for groundwater level applications and to test its efficiency on spatiotemporal analysis. Finally, the third goal was the calculation of spatiotemporal uncertainty that has not been approached before with a methodology based on classical Bayesian analysis.

Regarding the novelty of this work, it presents and asses two modified space-time variogram types using novel terms of physical meaning to model the space-time data dependence of groundwater level measurements. The first is a scale factor of hydraulic conductivity directional ratio and the second the hydraulic gradient. Moreover, it involves and tests the application of a non-Euclidean distance metric in the space-time geostatistical process. The procedure of defining the estimations uncertainty is also new as a Bayesian kriging type approach, using detrending and the bootstrap idea, is applied for the first time in joint space-time data. Finally, a combination of an exponentially weighted moving average filter with the Thiem's law, that define the groundwater flow under pumping of multiple wells to approximate the temporal groundwater level trend and to describe the corresponding spatial trend, is employed for the first time.

2.0 Spatiotemporal modelling: theory and application

The field application of the present work is related to Mires basin in the Messara watershed which is located on the island of Crete, Greece (Fig 1). The basin mainly consists of quaternary alluvial sediments which form an inter-bedded sequence of gravels, gravely sands, sands, silts, silty sands and clays. In its greatest extend the aquifer is homogeneous with only very small inconsistencies that exist in every aquifer. A small number of faults (four) exist at the center of the aquifer that may affect locally the groundwater flow. The hydraulic conductivity values are of the same magnitude 10^{-4} m/s in the entire aquifer. It varies thought from 0.0009 m/s in the East to 0.00021 m/s in the West. The basin's aquifer is characterized in the hydro-geological reports as unconfined. The mean annual rainfall in the basin is around 650 mm and the basin altitude is less than 300 m. About 65%

ACCEPTED MANUSCRIPT

of rainfall is lost to evapotranspiration and 10% as runoff to the sea, leaving only 25% to recharge the aquifer. The land use in the area comprise mainly of olive trees, vines, fruit trees, and vegetable cultivations (mostly open field and some greenhouses) (Varouchakis, 2016). Only 10 wells were regularly monitored between years 1981 and 2015, while groundwater level measurements were only taken bi-annually (wet-dry period) (Special water secretariat of Greece, 2015). Thus, the available data file consists of 680 values (34 bi-annual measurements implying 68 values at 10 monitoring stations) distributed in a matrix of 68 rows and 10 columns. The monitoring wells are unevenly distributed and mostly concentrated along Geropotamos River that crosses the basin.

Fig.1

Due to the overexploitation of the aquifer and the expeditious increase of drip irrigation, the water table has been declined almost 35 m since 1981, causing great shortage of the water resources in the area. The application of spatiotemporal geostatistics exploits the spatially short groundwater level dataset to determine the spatiotemporal variability of the aquifer and detect possible space-time interdependencies, useful for interpolation and extrapolation predictions.

Spatiotemporal geostatistical analysis considers the following steps: 1) approximation of spatiotemporal trend, 2) space-time variogram calculation, 3) application of space-time kriging, and 4) evaluation of the proposed methodology reliability by applying leave one out cross validation of the monitored data values, prediction at omitted onward time steps for validation purposes and calculation of estimations uncertainty i.e. space-time kriging variance and/or simulations. In this work the latter applied using a simulations technique in terms of space-time Empirical Bayesian Kriging. Space-time Ordinary kriging (STOK) and STRK are reliable methods for space-time estimation (Christakos et al., 2001; De Cesare et al., 2001; Varouchakis and Hristopulos, 2017). Nevertheless, the simultaneous solution of kriging equations to calculate the spatial and temporal

ACCEPTED MANUSCRIPT

weights of the system becomes complicated (Skøien and Blöschl, 2007). Thus, special attention is needed to ensure the validity and suitability of the chosen spatiotemporal dependence model. Therefore, first, the experimental spatiotemporal variogram is determined jointly in space and time according to the space-time classical moment estimator, $\hat{\gamma}_Z(\mathbf{r},\tau)=\frac{1}{2N(\mathbf{r},\tau)}\sum_{i=1}^{N}\sum_{j=1}^{N}\left[Z(\mathbf{s}_i,t_i)-Z(\mathbf{s}_j,t_j)\right]^2$, where, $\hat{\gamma}_Z(\mathbf{r},\tau)$ denotes the space-time variogram, $\mathbf{r}$ is the space lag and τ is the time lag. Then, separable and non-separable space-time variogram functions are fitted to the experimental space-time variogram using the Least Squares sum method to obtain the optimal theoretical variogram fit that will provide the space-time dependence parameters.

2.1 Geostatistical tools

The first step of a geostatistical analysis is to split the random function into two subcomponents, trend and fluctuations. The spatiotemporal trend considers separately the spatial and temporal trend under a product function. The product of the two trend types is inspired by the product covariance function that considers the multiplication of a purely spatial function and a purely temporal function to express the spatiotemoral data dependence. However, Kyriakidis and Journel (1999) have proposed a similar approach for the decomposition of trend and residuals of a Random Field.

An exponentially weighted moving average filter (EWMA) was applied on the mean bi-annual groundwater level field data to remove the average temporal trend of the groundwater level in the aquifer (Pham, 2006; Varouchakis and Hristopulos, 2017). The general form of EWMA model that is convenient in minimizing computations is applied in this work $\hat{m}_z(t_i)=w\,\overline{z(t_i)}+(1-w)\hat{m}_z(t_{i-1})$, with initial condition $\hat{m}_z(t_1)=z(t_1)$, where, $\hat{m}_z$ is the temporal trend, $\overline{z(t_i)}$ is the average groundwater level of the wells at the time t_i, and $0<w\leq 1$ is a constant weight determined by the data. The latter is a constant that determines how fast the exponential

ACCEPTED MANUSCRIPT

weights decline over the past consecutive periods. In its analytical form EWMA takes a weighted average of all past observations and use this as a forecast of the trend of a random variable at time t_i. Declining weights are put on older data by increasing the weight exponent during the smoothing process (Holt, 2004; Pham, 2006).

The spatial trend approximation is based on Thiem's equation that describes the groundwater flow when pumping in the aquifer is on (Varouchakis and Hristopulos, 2013). The form of the equation for an unconfined aquifer when multiple wells operate is given below (Bear, 1979; Todd, 1959),

$$H^2(\mathbf{s}) = H_0{}^2(\mathbf{s}) + \frac{1}{\pi K}\sum_{i=1}^{n} Q_i \ln\left(\frac{r_i}{R_i}\right), \quad r_i < R_i, \quad i = 1\ldots, n \quad (1)$$

where, $H(\mathbf{s})$ and $H_0(\mathbf{s})$ denote the estimated and initial groundwater levels at the point **s** respectively, K stands for hydraulic conductivity, r_i describes the distance between the prediction location and the contributing well **i**, n is the set of contributing wells, Q expresses the pumping rate, and R_i is the well's radius of influence in terms of an empirical equation (2) in the absence of available pumping tests (Bear, 1979; Todd, 1959).

$$R_i = 575\, s_{w,i} \sqrt{\hat{H}_{0,i}\, K_i} \quad (2)$$

In equation (2) $s_{w,i}$ corresponds to the groundwater drawdown at the well, and $\hat{H}_{0,i}$ (m) is the prior to pumping aquifer saturation thickness. Due to lack of information uniform values were used for the variables $s_{w,i}$ and K. An assumption was considered about $s_{w,i}$ due to different values that receives during the wet and dry period. The different pumping rates that occur during each season and the deviations from the agreed pumping rates according to the local authorities led to determine an average $s_{w,i}$ that corresponds to the mean annual drawdown of the aquifer level at each well.

ACCEPTED MANUSCRIPT

Thus, it was determined from a linear regression analysis of the mean annual groundwater level variations during a 34 years period at each well. The *K* value on the other hand was determined from a recent work that updated the hydraulic conductivity at the study area due to changes in the saturation thickness. The alluvial background of the aquifer provides *K values* of the same magnitude. The assigned values of *K* were spatially averaged from values obtained at different monitoring locations of the aquifer. The pumping rates were available as the 10 wells monitored in the area are registered in the national network with specified permitted pumping rates (Special water secretariat of Greece, 2015; Varouchakis, 2016).

Thiem's formulation meets in this work the application assumptions (Todd 1959, Bear 1979). The study aquifer is homogeneous as it consists of quaternary alluvial deposits, it has a hydraulic gradient from East to West equal to 0.004 (65-18 m /12000 m), denoting that prior to pumping conditions the aquifer level is almost horizontal, and equilibrium or steady state flow conditions have reached as the entire pumped water is yielded from external sources beyond the radius of influence, i.e. the radii of influence of the pumping wells are under 500 m, much less than the aquifer extend, which is around 12000 (m). In addition, the study aquifer receives inflows from the East and outflows to the West.

Thiem's equation is applied to approximate the spatial trend of the aquifer level separately at each timestep (wet and dry hydrological periods). The trend removal supports a more stable space-time variogram estimation that helps STRK to deliver results of improved accuracy. Steady state or equilibrium flow conditions apply at spatial scale within each specific timestep, along with the other Thiem equation application assumptions reported previously.

The product of the spatial trend, that follows the Thiem's law and the temporal trend that was calculated at every time step, was divided by a reference spatial trend component to provide the spatiotemporal trend variation. The latter is applied to keep the units in meters. The residuals

ACCEPTED MANUSCRIPT

calculated at every well at a specific time step were obtained as a result of the subtraction between the groundwater level and the spatiotemporal trend.

Groundwater level is part of the aquifer's saturation zone and describes the water table variation. Hydraulic conductivity is an important parameter that determines both groundwater flow and head in the saturation zone according to the basic groundwater flow equation expressed by the Darcy law (Bear, 1979). It is an anisotropic parameter that usually varies significantly in the vertical direction. Therefore, the average hydraulic conductivity directional ratio can be applied as a scale factor of the theoretical variogram model to control the fitting to the experimental variogram. The presence of outliers in datasets or of long spatiotemporal dependencies affect the range of the experimental variogram fluctuations and sill's location if any. Thus, the application of a scaling factor that has a physical meaning and directly affects groundwater level variations provides a consistent variogram fit that provides reliable parameters. A uniform hydraulic conductivity directional ratio was applied, as the aquifer porous media was characterized homogeneous by the hydrogeological studies conducted in the area. The application of such a scale factor, was inspired by a similar application of a global anisotropy ratio acting as a scale factor involving the vertical to horizontal hydraulic conductivity ratio to model the spatial variability of transmissivity (Chiles and Delfiner, 1999).

According to a hydrogeological literature review, the hydraulic conductivity follows the lognormal distribution with an exponential covariance (Desbarats, 1992). Similarly, the hydraulic head covariance of a simplified linear reservoir model appears to decrease with time and approaches the typical exponential covariance as time increases (Zhang and Li, 2005). On the other hand, at a local scale the hydraulic head is spatially interpreted by a differentiable function such as the basic groundwater flow equation. Thus, a differentiable covariance function, such as the Gaussian which is applicable and efficient in determining the spatial dependence of variations in small spatial resolutions, is considered to model the spatial dependence of the water table variations (Theodoridou et al., 2017). Therefore, considering the previous research findings and facts in the present work a Gaussian and an exponential variogram were applied. The first to describe the

ACCEPTED MANUSCRIPT

spatial dependence of the groundwater level residuals and the second the temporal. The experimental space-time variogram of the residuals was first calculated and then modelled with a theoretical spatiotemporal variogram function. Herein, the product-sum spatiotemporal variogram was applied by means of the Gaussian and the exponential variogram functions:

$$\gamma_{z_s}(\mathbf{r}) = \frac{K_z}{K_{x,y}}\sigma^2_{z_s}\left[1-\exp\left(-\frac{|\mathbf{r}_s|}{\xi_s}\right)^2\right] \quad (3)$$

$$\gamma_{z_t}(r_t) = \frac{K_z}{K_{x,y}}\sigma^2_{z_t}\left[1-\exp\left(-\frac{|r_t|}{\xi_t}\right)\right] \quad (4)$$

where σ is the variance, ξ is the correlation length in space (s) and time (t), $\mathbf{r}$ is the lag vector in space and time and the K fraction is the hydraulic conductivity directional ratio . The product-sum variogram combines the use of separate spatial and temporal variograms under a non-separable function. The product-sum space-time variogram (De Cesare et al., 2001) model is inspired from the separate product and sum models. It is defined as:

$$C_{ST}(\mathbf{r}_s, r_t) = k_1 C_S(\mathbf{r}_s) C_T(r_t) + k_2 C_S(\mathbf{r}_s) + k_3 C_T(r_t) \quad (5).$$

C_S, C_T are purely spatial and temporal covariance models with $k_1 > 0$, $k_2 \geq 0$, $k_3 \geq 0$. In terms of the variogram, the above equation is expressed as:

$$\gamma_{ST}(\mathbf{r}_s, r_t) = \left(k_1 C_S(0) + k_3\right)\gamma_T(r_t) + \left(k_1 C_T(0) + k_2\right)\gamma_S(\mathbf{r}_s) - k_1\gamma_S(\mathbf{r}_s)\gamma_T(r_t) \quad (6),$$

where γ_S, γ_T are purely spatial and temporal variogram models.

ACCEPTED MANUSCRIPT

On the other hand, Spartan covariance and variogram functions that were introduced by Hristopulos (2003) and have been implemented to miscellaneous environmental data sets (Elogne et al., 2008; Elogne and Hristopulos, 2008; Hristopulos, 2003; Hristopulos and Elogne, 2009; Varouchakis and Hristopulos, 2013; Varouchakis and Hristopulos, 2017) were also applied in this work. Herein, this family of functions is modified appropriately to model hydro-geological data. The Spartan covariance functions in $d = 3$ dimensions are expressed as follows:

$$C_z(\mathbf{h}) = \begin{cases} \dfrac{\eta_0\, e^{-h\beta_2}}{2\pi\sqrt{|\eta_1^2-4|}}\left[\dfrac{\sin(h\beta_1)}{h\beta_1}\right], & \text{for } |\eta_1|<2,\ \sigma_z^2=\dfrac{\eta_0}{2\pi\sqrt{|\eta_1^2-4|}} \\ \dfrac{\eta_0\, e^{-h}}{8\pi}, & \text{for } \eta_1=2,\ \sigma_z^2=\dfrac{\eta_0}{8\pi} \\ \dfrac{\eta_0\,(e^{-h\omega_1}-e^{-h\omega_2})}{4\pi(\omega_2-\omega_1)\,h\sqrt{|\eta_1^2-4|}}, & \text{for } \eta_1>2,\ \sigma_z^2=\dfrac{\eta_0}{4\pi\sqrt{|\eta_1^2-4|}} \end{cases} . \qquad (7)$$

where, η_0 is the scale factor, η_1 is the rigidity coefficient, $\beta_1 = |2-\eta_1|^{1/2}/2$ is a dimensionless wavenumber, $\beta_2 = |2+\eta_1|^{1/2}/2$ and $\omega_{1,2} = \left(|\eta_1 \mp \Delta|/2\right)^{1/2}$, $\Delta = |\eta_1^2-4|^{1/2}$, ξ stands for the correlation length, $\mathbf{h} = \mathbf{r}/\xi$ is the normalized lag vector, $h = |\mathbf{h}|$ is the separation distance norm, while σ_z^2 is the variance.

Equation (7) can be also allied in two dimensions, (Christakos, 1991). In case of $\eta_1 = 2$ the covariance is expressed by the exponential model, while for $|\eta_1| < 2$ by the combination of the exponential and hole-effect. The respective stationary variogram model is then given by $\gamma_{ST}(\mathbf{r}_s, r_t) = \sigma_z^2 - C_z(\mathbf{h})$.

The spatiotemporal Spartan function constitutes a new approach in the interdependence modeling of spatiotemporal data (Varouchakis and Hristopulos, 2017). It forms a non-separable model, which is derived by substituting *h* with the following equation in its spatial form of equation (7),

ACCEPTED MANUSCRIPT

$\mathbf{h} = \sqrt{\mathbf{h}_r^2 + \alpha\,\mathbf{h}_\tau^2}$, $\mathbf{h}_r = \frac{r}{\xi_r}$, $\mathbf{h}_\tau = \frac{\tau}{\xi_\tau}$, where τ is the time step lag and α denotes a relative weight of the time lag with respect to the spatial lag. The scale factor η_0 that partly defines the variance of the variogram is expressed in terms of the average spatiotemporal hydraulic gradient ($\eta_0^{dh/dl}$) of the space-time groundwater level dataset. The latter is applied to obtain a physical parameter in the function that determines the highest value (sill) of the measurement variable in terms of different spatial and temporal separation distances. A similar approach is common in developing covariance structures of physical meaning by including a parameter that affects the spatial or temporal behavior of the measured variable (Kolovos et al., 2004). Both variograms developed in this work are valid variogram functions as they satisfy the conditions of Bochner's theorem i.e. the Fourier transform exist and is non-negative (De Cesare et al., 2001; Varouchakis and Hristopulos, 2017).

The spatiotemporal process is anisotropic because of the time dimension enclosure. The product-sum space-time variogram was applied likewise to other works of similar topic using isotropic variograms for space and time correlations (De Iaco, 2010; Raja et al., 2017; Tadić et al., 2017). However, the application of separate variogram models for space and time that have a different sill under the same space-time joint function means the incorporation of zonal anisotropy (Hoogland et al., 2010). Geometric anisotropy on the other hand can be comprised when a common term of correlation length applies in a variogram function. Then, it is appropriately modified using an anisotropic ratio parameter to approximate the difference of the spatial to temporal scale (Hoogland et al., 2010), which in our case it was possible to be only applied for the Spartan type. Thus, it was applied modifying the correlation length in equation (7).

Another new approach in the modeling of spatiotemporal data is the application of non-Euclidean distance metrics. In the present study, the Manhattan metric, described by equation (8), is applied to examine the effect of distance calculation on the data interdependence modelling and the prediction results:

ACCEPTED MANUSCRIPT

Manhattan: $d_1 = |x_i - x_j| + |y_i - y_j|$ (8)

where, the Cartesian coordinates of the i[th] and j[th] monitoring points (wells) are expressed by (x_i, y_i), (x_j, y_j), $i, j \in 1,..,n$, in the area of study and n is the number of wells. In case of grid-path data, the application of Manhattan distance provides better results due to its concentric rhombus structure compared to Euclidean distance whose formula describes a concentric circle. Due to this special feature, the aforementioned distance has the ability to bypass spatial hydrogeological discontinuities between the measurements (Theodoridou et al., 2017).

Then, STRK is applied to combine both the residuals and the trend interpolation, while the empirical Bayesian bootstrap method (Pilz and Spöck, 2008) was applied to determine the overall uncertainty of estimations. This stochastic modelling approach is based on the Monte Carlo simulation approach and produces multiple realizations, rank the prediction results with respect to specified criteria, and captures the range of the uncertainty. The process considers the following steps:

- Unconditional simulation of the field space-time fluctuations at the monitoring locations using the estimated model statistics and superposition with estimated trend. The unconditional simulation process replicates the data mean, variance, and variogram (on average).
- Estimation of the spatial and temporal groundwater level trend for the simulated realization and of the associated parameters using the same trend model structure.
- Estimation of the empirical space-time residuals variogram and model fitting.
- Iteration of the above steps, e.g. 1,000 times, leads to the posterior distribution of the space-time model parameters (empirical Bayesian bootstrap idea).
- For each realization, STRK was performed to estimate the head at the nodes of a 100 × 100

ACCEPTED MANUSCRIPT

grid for a specified time step of the study period (herein bi-annually) leading to the predictive distribution.

- At each grid point the mean CDF (cumulative distribution function) as well as the 5% and 95% CDF quantiles were calculated.

Using Bayes theory one can acquire a posteriori distribution of parameters using the prior distribution and the initial values of the parameters. In Bayesian kriging the posterior distribution of the parameters involved (trend model and variogram) is specified by means of simulations, which corresponds to their uncertainty. In order to implement Bayesian kriging method, first the appropriate space-time variogram model of the fluctuations is determined after fitted to the experimental one. The fluctuations were obtained by removing the spatiotemporal trend from the initial dataset. Using the parameters derived and the variogram function, the covariance matrix is constructed. Then, uniform random numbers generation is applied (see Appendix). These correlated random values have the same statistical characteristics with the initial observations' dataset. Besides, the random values represent a new realization that first undergoes detrending, then the variogram of the fluctuations is calculated and finally STRK is applied to estimate values at unknown locations. This procedure is performed iteratively as described at the steps previously presented. Therefore, aquifer level and prediction uncertainty maps can be developed to present the groundwater level distribution based on the spatiotemporal interdependence of the available data.

To determine the spatiotemporal variability of Mires aquifer's groundwater level since 1981 and to use the data correlations to undertake predictions, a spatiotemporal geostatistical analysis, based on the aforementioned tools, was performed. Two validation methods were applied to test the spatiotemporal model capabilities. First the spatiotemporal experimental variogram was calculated using bi-annual groundwater level data from the ten sampling locations for the period 1981-2014. Validation of the estimates was performed using bi-annual data of the wet and dry periods for the year 2014-2015. The available dataset consists of bi-annual measurements from 1981 to 2015. A

ACCEPTED MANUSCRIPT

spatiotemporal variogram needs a sufficient time period and number of data in order to effectively represent the interdependence of the available measurements and to capture the data variability. Usually, in spatiotemporal analysis the predictive capability of the model is tested (Sakizadeh et al., 2019; Tapoglou et al., 2014; Varouchakis, 2017; Varouchakis and Hristopulos, 2017). Thus, the spatiotemporal dependence of the dataset values was determined using the entire available data information apart from the last hydrological year in order to assess the prediction capability of the proposed model at the monitoring locations for the dry and wet period where measurements occur.

On the other hand, the entire dataset was used with the proposed model via a leave one out cross validation to assess the estimation capability of the model at ungauged locations. Apart from the classical estimation metrics, absolute error and absolute relative error, two more metrics are applied to assess the efficiency of the proposed methodologies. The root mean square standardized error RMSSE (Diodato, 2005) and the modified Index of Agreement (IoA′) (Calzolari and Ungaro, 2012). The root mean square standardized error (RMSSE) compares the error variance with a theoretical variance, such as kriging variance. Therefore, it should be close to unity, if the RMSSE is greater than one, the prediction variability is underestimated by the kriging variance, whereas if RMSSE is less than one, the variability is overestimated. In this work we apply a complex spatiotemporal trend model and a simulation approach to capture the overall uncertainty considering the space-time kriging parameters involved as well. Therefore, we assess the RMSSE for the calculated residuals.

$$\varepsilon_{RMSS} = \sqrt{\frac{1}{N}\sum_{i=1}^{N}\left[\frac{z^{*}(\mathbf{s}_i) - z(\mathbf{s}_i)}{\hat{\sigma}(\mathbf{s}_i)}\right]^2} \quad (9)$$

where, $z^{*}(\mathbf{s}_i)$ is the estimated head at point $\mathbf{s}_i$, $z(\mathbf{s}_i)$ is the observed head and $\hat{\sigma}^2(\mathbf{s}_i)$ is the kriging variance. On the other hand, the modified Index of Agreement (IoA′) ranges between 0 and 1, is a

ACCEPTED MANUSCRIPT

standardized measure of the mean error and expresses the agreement directly; the optimal value is 1 (Calzolari and Ungaro, 2012),

$$IoA^{'} = 1 - \frac{\sum_{i=1}^{N} \left| z(\mathbf{s}_i) - z^{*}(\mathbf{s}_i) \right|}{\sum_{i=1}^{N} \left(\left| z^{*}(\mathbf{s}_i)_i - \overline{z(\mathbf{s}_i)} \right| + \left| z(\mathbf{s}_i) - \overline{z(\mathbf{s}_i)} \right| \right)} \quad (10)$$

where, $\overline{z(\mathbf{s}_i)}$ denotes the average of the observed data.

3.0 Results and Discussion

Following, the proposed spatiotemporal trend analysis and the space-time variogram of the residuals were applied. The optimal EWMA coefficient was determined w=0.71 from the temporal trend fitting process. The experimental variogram fitting to the proposed product-sum spatiotemporal model and the associated parameters are presented in Fig. 2. The hydraulic conductivity directional ratio for the study area was based on the available hydrogeological information that decreases in the vertical direction by an order of magnitude compared to the horizontal direction, K_z=0.000057m/s and $K_{x,y}$=0.00057m/s. Next, a validation process was applied using STRK to identify the efficiency of the estimations. The validation results, in terms of the Absolute Error (AE) and Absolute Relative Error (ARE) are presented in Table 1. Figure 2 presents the fitting of the theoretical modified Spartan space-time variogram model to the corresponding experimental variogram and the respective variogram parameters. The average spatiotemporal hydraulic gradient was calculated equal to dh/dl=0.08m. The nugget term was considered to improve the experimental variogram fit. The validation results of the latter approach are also presented in Table 1. The first four columns present the groundwater level estimation error for the wet and dry period of hydrological year 2014-2015 using STRK and the product-sum variogram,

ACCEPTED MANUSCRIPT

while the last four columns represent the corresponding error using STRK and the Spartan type variogram. Both approaches involve the application of the Manhattan distance metric.

Table 1 STRK estimates absolute error (AE) and absolute relative error (ARE) for the wet and dry period of the year 2014-15 using the product-sum type variogram and the Spartan type variogram.

Well No	Wet period product-sum		Dry Period product-sum		Wet period Spartan		Dry Period Spartan	
	AE (m)	ARE %	AE (m)	ARE %	AE (m)	ARE %	AE (m)	ARE %
G1	1.39	6.20	1.60	7.50	1.02	4.21	1.38	5.80
G2	1.18	5.10	1.50	6.40	0.95	3.50	1.29	4.20
G3	0.84	5.40	1.09	6.10	0.81	4.60	0.94	5.10
G4	1.40	4.60	1.55	6.80	1.27	3.80	1.34	4.60
G5	1.53	2.80	1.66	4.20	1.21	1.50	1.43	3.10
G6	1.21	3.10	1.44	4.90	1.01	1.82	1.24	2.90
G7	0.97	4.10	1.10	5.80	0.77	2.30	0.95	4.20
G8	1.10	5.30	1.15	6.60	0.93	3.40	0.99	3.40
G9	0.79	3.90	0.97	4.60	0.61	1.21	0.84	3.10
G10	0.85	2.50	1.11	3.40	0.77	1.37	0.96	2.70

Fig.2

Neither of the variograms has an actual correlation length since their fit is only asymptotic to the sill, in these cases it is common to refer to the effective range i.e. the lag distance at which the variogram value is 95% of the sill. The space-time variogram parameters provide useful information for the dataset, sampling and the aquifer physical characteristics. The variance parameters denote the variance of the variable studied and the sill or approximated sill of the theoretical model. The sill of both variograms is similar denoting consistency, in absolute units around 6.5 m, meaning that the spatiotemporal groundwater level variations at the aquifer indicate medium scale fluctuations from the mean value that depend on the extensive aquifer pumping. Both variograms exhibit a nugget effect that signifies measurement errors or spatiotemporal variations at smaller scale than the

ACCEPTED MANUSCRIPT

sampling interval or both. In this work the nugget effect depends on the scarce available dataset, 10 spatial monitoring locations in bi-annual scale that cannot capture small scale variations spatially and temporarily. The correlation length (effective range) parameter for both variogram types denote long spatial dependences due to the aquifer hydrogeological homogeneity, but small-scale temporal dependences due to the unregulated pumping that occur over time in the aquifer. Finally, the other calculated variogram parameters as explained in the methodology section are shape coefficients that help the variogram fitting procedure.

Spatial and temporal trends were significant in the available dataset. Before detrending the experimental variogram was characterized by important fluctuations, while after detrending residuals delivered a smoother experimental variogram that can partially reach a sill. Both detrending methods were consistent as they provided residuals that deliver variograms of similar shape for the produced realizations of the simulation procedure. In addition, both STRK models assessed in this work were consistent as they produced similar patterns of groundwater level spatial distribution in the study aquifer.

As it is shown in Tables 1 and 2 STRK provides a very good agreement with the reported values to be improved by 18% on average in terms of absolute error compared to the previous methodology involving the product-sum variogram. In addition, STRK estimates are improved by 22% when the modified Spartan model is applied as well as the Manhattan distance compared to the Euclidean, and by 40% compared to STOK using the original Spartan variogram and the Euclidean distance metric. In this work the Manhattan distance metric applies better compared to the Euclidean distance in connecting locations due to the presence of faults in the study aquifer (Fig. 1) that can be bypassed because of the grid path that it follows.

Table 2 Comparison of the performance of the models tested in terms of mean absolute error (MAE) and mean absolute relative error (MARE) for the wet and dry period of the year 2014-15.

Method	**MAE (m)**	**MARE %**
Space-time regression kriging / Spartan variogram / Manhattan distance	1.03	3.30
Space-time regression kriging / Product-sum variogram /	1.22	5.00

ACCEPTED MANUSCRIPT

Manhattan distance		
Space-time regression kriging / Spartan variogram / Euclidean distance	1.25	6.70
Space-time ordinary kriging / Spartan variogram / Euclidean distance	1.44	9.10

On the other hand, RMSSE estimate for the optimal approach is equal to 0.94, thus close to 1.00, implying that STRK with the modified Spartan variogram and the Manhattan distance metric deliver reliable estimates with kriging variance representative of prediction uncertainty. The approach that involves the product-sum variogram delivers an RMSSE equal to 0.88 providing also reliable results. The IoA′ for the STRK using the modified Spartan variogram is equal to 0.91, while using the product-sum function equal to 0.80. Both, IoA′ values denote estimations of significant accuracy, but with the first model approach to prevail.

Finally, interpolation maps were derived using the Bayesian STRK type. Therefore, aquifer level maps for the 2014-2015 hydrological year were then derived using the modified Spartan spatiotemporal variogram structure and the Manhattan distance metric. The maps presented the aquifer level variations during the wet and dry period accompanied by the estimated uncertainty (Figs. 3 and 4). To construct the maps produced by the geostatistical analysis, the estimates are kept within the interpolation area. The 2D plots are accompanied by additional plots (Figs. 5 and 6) showing two cross sections of the study aquifer. The additional plots include the aquifer level distribution during the wet and dry period in the study area as well as hydrogeological and topographic information that help the results to be better interpreted. The wells with the lower and higher uncertainty bounds are presented in the attached cross sections, highlighting that the lower estimation uncertainty was met at wells close to the measurements core and higher in those further away.

Fig. 3

Fig. 4

ACCEPTED MANUSCRIPT

Fig. 5

Fig. 6

Another indicator to assess the reliability of the optimal method is the posterior distribution of the parameters involved. The posterior distribution of the most important parameters of the space-time trend model and of simulated variograms are presented in Figure 7. The posterior parameters distribution is close to normal, fact that strengthens the methodology and results validity and reliability.

Fig. 7

A classical leave one out cross validation procedure (Olea, 1999) was also applied to test the estimation capability of the proposed method using the entire dataset this time. STRK using the modified Spartan variogram and the Manhattan distance metric displayed estimates of significant accuracy as the absolute average error was equal to 1.81 m and the mean absolute relative error 0.09. On the other hand, STRK using the product-sum variogram and the Manhattan distance metric also delivered results of significant accuracy with an absolute average error equal to 2.51 m and a mean absolute relative error of 0.11. STOK provided an absolute average error equal to 3.71 m and a mean absolute relative error of 0.15. The observed values vary spatially form East to West. The hydraulic gradient might be small, but the model must predict values in the range of 65 m to 18 m. At temporal scale the fluctuations may vary from 2 m to 6.5 m seasonally and from 0.5 m to 3 m annually. Therefore, the proposed model has the ability to provide estimates of significant accuracy and consistency.

At ungauged locations, the proposed model is expected to provide reliable estimates considering its estimation capability. The space-time kriging variance of the residuals shows the expected spatial

ACCEPTED MANUSCRIPT

distribution of uncertainty at ungauged locations. Away from the measurements locations the uncertainty increases and becomes highest at the boundaries of the area where there are no measurements. Figure 8 presents the average standard deviation of estimated residuals for all time-steps using the proposed STRK model. The estimated kriging standard deviation range is low due to the precise theoretical space-time variogram fit to the experimental one, which declares accurate parameters estimation. However, for STRK applications, that involve complex trend functions, the full uncertainty estimation should involve a simulation approach.

Fig. 8

The groundwater spatial variability estimation in an aquifer using a scarce dataset as herein influences the presence of high estimation error and uncertainty. However, the application of an appropriate trend approximation technique and of a spatiotemporal dependence function can reduce the estimations error and uncertainty. Nevertheless, in such cases the space-time kriging variance is not appropriate to express the uncertainty of estimations as the spatiotemporal uncertainty depends also on the effect of the spatiotemporal trend model parameters that are involved. This work does not employ a standard space-time regression kriging method with known standard predictors e.g. elevation and/or coordinates to calculate the space-time regression kriging variance (Hengl et al., 2007). It applies space-time residual kriging where the auxiliary information is obtained through equations that express the groundwater process in space and time and involve several parameters that contain uncertainty. Thus, in such cases simulations (Figs. 3 and 4) apply to quantify the uncertainty of estimations (Bierkens et al., 2001; Pilz and Spöck, 2008) within specific quantiles that determine the estimations uncertainty bounds.

Apart from the exponential moving average model weight parameter and the space-time variogram parameters a number of variables are involved for the calculation of the spatial trend. The radius of influence is determined from the drawdown at each well which is calculated as the average annual

ACCEPTED MANUSCRIPT

drawdown the last 34 years, while hydraulic conductivity due to the homogeneous aquifer receives a specific characteristic value. The proposed model has a reduced estimation error compared to the other models tested (Table 2) and estimations uncertainty that consider the uncertainty of all the involved space-time model parameters. However, the estimations uncertainty is lower compared to STOK by 22%, implying that the estimated fluctuations were more stable, as expected, and were modeled effectively by the spatiotemporal variogram function. In addition, this implies that the assigned variable values were reliable and characteristic for the case study.

The range of spatiotemporal variability of the estimated uncertainty is low for estimation points close to measurement points and inside the radius of influence of wells that have a drawdown close to the estimated average. Its extent depends more on the trend model parameters and variables and less on the variogram parameters because the estimated residuals provide a stable experimental variogram that fits efficiently to the theoretical model.

The scope of this work was to employ two new tools of physical background in the variogram calculation of the available data and to test their efficiency for modeling the spatiotemporal response of the groundwater level variations in an aquifer. The proposed tools delivered excellent variogram fits with very accurate estimates. However, for the most accurate approach that involved the modified Spartan variogram the spatial and temporal correlation lengths (effective ranges) were calculated approximately equal to 3 km and 12 months, respectively. The temporal range denotes that the spatiotemporal prediction considers measurements of both (wet and dry) hydrological periods. Therefore, according to Rouhani and Myers (1990) the model is capable to provide consistent estimates during dry and wet periods. In Rouhani and Myers (1990) is stated that if only data from a dry period are used the space-time kriging estimates in wet period would not be reliable and vice versa. In addition, if a correlation length in time considers only dry or wet period observations then estimates are only reliable for the specific period type. The available dataset is at bi-annual scale (wet-dry period) for 34 years. Therefore, a temporal correlation length of 12 months is short compared to the length of the time series. Furthermore, a 12-month correlation length

ACCEPTED MANUSCRIPT

expresses a temporal variability within one year as it considers wet and dry period observations. Moreover, it means that temporal observations within one year are correlated to each other.

A large number of unregistered wells are operating in the study area. Depending on how wet/dry a year is and on the availability of surface waters, pumping rates may increase/decrease compared to the registered wells. The aquifer recharge, depending on the hydrological year type (wet or dry), does not replenish regularly the aquifer. Therefore, the aquifer groundwater level does not remain stable during the monitoring period to provide long temporal dependencies. It fluctuates with a decreasing trend. The groundwater level of the aquifer varies at annual scale due to the unregulated pumping of the unregistered wells. The groundwater level is mostly closer to the previous timestep value of 12 months range either for wet or for dry period exactly as determined by the correlation length. Thus, short temporal groundwater level dependencies occur in the aquifer. Figures 3 and 4 present the spatial variability of the estimated groundwater level based on the space-time correlations of the data that consider the dynamic aquifer behavior.

The Manhattan distance metric provides improved predictions. This may result from the physical characteristics of the aquifer. Manhattan distance metric compared to the Euclidean distance has the ability to estimate the distance between two points accordingly to the axes orientation. Thus, in the case of a geological discontinuity exists (e.g. a karstic or fracture intervention), the Manhattan function is the appropriate metric to calculate the distance between two points. However, it is worth mentioning that the aforementioned approach is not necessarily the appropriate for each data set, but it depends on the characteristics of the system under study and on the scope of each study.

The proposed scaling factors of physical background provide more stable theoretical variograms with an excellent fit to the experimental variogram leading to optimal parameter calculation for the prediction process with STRK. Therefore, the proposed variograms are flexible new models for the estimation of the interdependence of groundwater level space-time data. In addition, STRK by using the modified variogram structure provided accurate results. In comparison to the classic

ACCEPTED MANUSCRIPT

STOK the involvement of a physical law in the trend function, that supports the secondary information, improves the interpolation accuracy. Finally, it was clearly identified that the contribution of the Bayesian Bootstrap idea was significant for the assessment of the spatiotemporal model parameter uncertainty and for the aquifer level estimates.

4.0 Conclusions

The understanding of the hydraulic head spatiotemporal variability derived from reliable estimation processes is vital to the water resources management. This work presented the space-time geostatistical analysis framework and examined the spatiotemporal modeling of groundwater level in a sub-surface aquifer where the groundwater resources have been significantly depleted the past 35 years. Two modified space-time variogram functions were presented and successfully tested in this work involving terms such as the hydraulic conductivity directional ratio and the hydraulic gradient with an objective to model the space-time dependence of the groundwater level variations. The optimal spatiotemporal approach employed the application of the Spartan variogram function involving the term of hydraulic gradient to approximate the scale parameter of the space-time variogram. This spatiotemporal structure models closely the experimental space-time variogram of the groundwater level residuals after effective detrending, capturing the space-time correlations of the available data. Both variogram models provided long spatial dependencies explained by the aquifer homogeneity, while short temporal dependencies exist due to the aquifer level variations through the years. STRK joint by the proper spatiotemporal trend model, distance metric and interdependence functions establish a reliable and flexible approach for the stochastic modeling of sparse groundwater level data. The proposed methodology employed a new space-time trend model, which approximates both the temporal and spatial trends. Even though this idea it is not new, the description of the temporal trend by an exponentially weighted moving average filter and the involvement of a groundwater flow physical law in the spatial term are applied for the first time.

ACCEPTED MANUSCRIPT

The trend function reduces efficiently the measurement trend leading to a smooth space-time variogram structure, while affects, more than the geostatstical method, the estimations uncertainty due to a sufficient number of parameters and variables involved. The STRK estimates presented accurately the groundwater level variability delivering accurate cross validation and prediction results, while provided the spatial distribution of the aquifer level at ungauged locations for the wet and dry period of the year 2014-2015. The examined approach accompanied by the Bayesian bootstrap idea provides estimations of improved uncertainty and establishes a useful assessment tool of aquifer level spatiotemporal variation for spatiotemporal aquifer level modeling in the absence of detailed hydrogeological data. The proposed methodology was applied and tested under the specific aquifer properties, characteristics and available data. The authors have focused on the analytical presentation of the methodology steps and capabilities in case one would like to transfer it in an aquifer of similar behavior and properties.

Acknowledgments

The authors would like to thank the editor and the three anonymous reviewers for their effort to provide constructive suggestions for the improvement of this work.

Appendix

A generally approved method of correlating random numbers, with a known covariance matrix (C), is by finding a matrix U, according to equation (11).

$$U^T \cdot U = C \quad (11)$$

Matrix U is a triangular matrix and can be derived using decomposition methods. Matrix decomposition is commonly used in Monte Carlo method for simulating systems with multiple

ACCEPTED MANUSCRIPT

correlated variables. Using this matrix, correlated random numbers R_c can be generated from uncorrelated numbers R, equation (12).

$$R_c = R \cdot U \quad (12)$$

Cholesky decomposition is one way of providing these random correlated values. The covariance matrix of a vector X can be given as $C = E(XX^T)$. If X is a random vector, consisting of uncorrelated random values uniform in [0,1], then $E(XX^T) = I$. The Cholesky decomposition of a covariance matrix is given as $C = L \cdot L^T$; it is possible to obtain a Cholesky decomposition of C since by definition the covariance matrix C is symmetric and positive definite. When the random vector X is multiplied by L ($Z = L \cdot X$), the following statement applies,

$$E(ZZ^T) = E\big((LX) \cdot (LX)^T\big) = E(LX \cdot X^T L^T) = L \cdot E(X \cdot X^T) \cdot L^T = L \cdot I \cdot L^T = L \cdot L^T = C\,, \quad (13)$$

denoting that, the random vector Z has the statistical properties of the initial dataset. The distribution of the simulated values using STRK can be used to derive the confidence intervals of the estimation process and to determine the posterior parameters distribution. Both reflect to the uncertainty of the proposed model.

References

ACCEPTED MANUSCRIPT

An, Y., Lu, W., Cheng, W., 2015. Surrogate Model Application to the Identification of Optimal Groundwater Exploitation Scheme Based on Regression Kriging Method—A Case Study of Western Jilin Province. Int. J. Environ. Res. Public Health 12(8), 8897-8918.

Aryaputera, A.W., Yang, D., Zhao, L., Walsh, W.M., 2015. Very short-term irradiance forecasting at unobserved locations using spatio-temporal kriging. Solar Energy 122, 1266-1278. DOI:https://doi.org/10.1016/j.solener.2015.10.023

Asher, M.J., Croke, B.F.W., Jakeman, A.J., Peeters, L.J.M., 2015. A review of surrogate models and their application to groundwater modeling. Water Resour. Res. 51(8), 5957-5973. DOI:10.1002/2015wr016967

Baú, D.A., Mayer, A.S., 2006. Stochastic management of pump-and-treat strategies using surrogate functions. Adv. Water Resour. 29(12), 1901-1917. DOI:https://doi.org/10.1016/j.advwatres.2006.01.008

Bear, J., 1979. Hydraulics of groundwater. McGraw-Hill, New York.

Bierkens, M.F.P., Knotters, M., Hoogland, T., 2001. Space-Time Modeling of Water Table Depth Using a Regionalized Time Series Model and the Kalman Filter. Water Resour. Res. 37(5), 1277-1290.

Calzolari, C., Ungaro, F., 2012. Predicting shallow water table depth at regional scale from rainfall and soil data. J. Hydrol. 414–415(2012), 374-387.

Chaojun, G., Yang, D., Jirutitijaroen, P., Walsh, W.M., Reindl, T., 2014. Spatial Load Forecasting With Communication Failure Using Time-Forward Kriging. IEEE Trans. Power Syst. 29(6), 2875-2882. DOI:10.1109/TPWRS.2014.2308537

Chiles, J.P., Delfiner, A., 1999. Geostatistics (modeling spatial uncertainty). Wiley, New York.

Christakos, G., 1991. Random field models in earth sciences. Academic press, San Diego.

Christakos, G., 2000. Modern Spatiotemporal Geostatistics. Oxford University Press, New York.

ACCEPTED MANUSCRIPT

Christakos, G., Bogaert, P., Serre, M.L., 2001. Temporal GIS: Advanced functions for field-based applications, 1. Springer Verlag, Berlin.

Christakos, G., Hristopulos, D.T., 1998. Spatiotemporal environmental health modelling: A tractatus stochasticus. Kluwer, Boston.

Cressie, N., 1993. Statistics for spatial data (revised ed.). Wiley, New York, 900 pp.

Cressie, N., Huang, H.C., 1999. Classes of Nonseparable, Spatio-Temporal Stationary Covariance Functions. J. Am. Stat. Assoc. 94(448), 1330-1340.

De Cesare, L.D., Myers, D.E., Posa, D., 2001. Estimating and modeling space-time correlation structures. Stat. Probabil. Lett. 51(1), 9-14.

De Iaco, S., 2010. Space-time correlation analysis: A comparative study. J. Appl. Stat. 37(6), 1027-1041.

Desbarats, A.J., 1992. Spatial averaging of hydraulic conductivity in three-dimensional heterogeneous porous media. Math. Geol. 24(3), 249-267. DOI:10.1007/BF00893749

Desbarats, A.J., Logan, C.E., Hinton, M.J., Sharpe, D.R., 2002. On the kriging of water table elevations using collateral information from a digital elevation model. J. Hydrol. 255(1-4), 25-38.

Dimitrakopoulos, R., Luo, X., 1994. Spatiotemporal modeling: covariances and ordinary kriging systems. Geostatistics for the Next Century. Kluwer, Dordrecht, 88–93 pp.

Diodato, N., 2005. The influence of topographic co-variables on the spatial variability of precipitation over small regions of complex terrain. Int. J. Climatol. 25(3), 351-363. DOI:doi:10.1002/joc.1131

Elogne, S., Hristopulos, D., Varouchakis, E., 2008. An application of Spartan spatial random fields in environmental mapping: focus on automatic mapping capabilities. Stoch. Env. Res. Risk A. 22(5), 633-646.

Elogne, S.N., Hristopulos, D.T., 2008. Geostatistical applications of Spartan spatial random fields. In: Soares, A., Pereira, M.J., Dimitrakopoulos, R. (Eds.), geoENV VI - Geostatistics for

ACCEPTED MANUSCRIPT

environmental applications in series: Quantitative geology and geostatistics. Berlin, Gemany: Springer, pp. 477-488.

Giraldo Henao, R., 2009. Geostatistical analysis of functional data. PhD Thesis, Universitat Politechnica de Catalunya, Barcelona.

Gneiting, T., 2002. Nonseparable, stationary covariance functions for space-time data. J. Am. Stat. Assoc. 97(458), 590-600.

Gneiting, T., Genton, M.G., Guttorp, P., 2007. Geostatistical space-time models, stationarity, separability, and full symmetry. In: Finkenstaedt, B., Held, L., Isham, V. (Eds.), Monographs On Statistics and Applied Probability. Chapman & Hall/CRC Press, Boca Raton, Florida, pp. 151-175.

Hengl, T., Heuvelink, G.B.M., Perčec Tadić, M., Pebesma, E.J., 2011. Spatio-temporal prediction of daily temperatures using time-series of MODIS LST images. Theor. Appl. Climatol. 107(1-2), 1-13.

Hengl, T., Heuvelink, G.B.M., Rossiter, D.G., 2007. About regression-kriging: From equations to case studies. Comput. Geosci. 33(10), 1301-1315.

Heuvelink, G.B.M., Griffith, D.A., 2010. Space–Time Geostatistics for Geography: A Case Study of Radiation Monitoring Across Parts of Germany. **地理学的**时空地统计学：横跨德国部分区域的辐射监测的案例研究. Geogr. Anal. 42(2), 161-179. DOI:10.1111/j.1538-4632.2010.00788.x

Hill, M.C., 2006. The Practical Use of Simplicity in Developing Ground Water Models. Groundwater 44(6), 775-781. DOI:10.1111/j.1745-6584.2006.00227.x

Holt, C.C., 2004. Forecasting seasonals and trends by exponentially weighted moving averages. Int J. Forecast. 20(1), 5-10. DOI:https://doi.org/10.1016/j.ijforecast.2003.09.015

Hoogland, T., Heuvelink, G.B.M., Knotters, M., 2010. Mapping water-table depths over time to assess desiccation of groundwater-dependent ecosystems in the Netherlands. Wetlands 30(1), 137-147.

ACCEPTED MANUSCRIPT

Hristopulos, D.T., 2003. Spartan Gibbs random field models for geostatistical applications. Siam J. Sci. Comput. 24(6), 2125-2162.

Hristopulos, D.T., Elogne, S.N., 2009. Computationally efficient spatial interpolators based on Spartan spatial random fields. IEEE Trans. Signal Process. 57(9), 3475-3487.

Júnez-Ferreira, H.E., Herrera, G.S., 2013. A geostatistical methodology for the optimal design of space–time hydraulic head monitoring networks and its application to the Valle de Querétaro aquifer. Environ. Monit. Assess. 185(4), 3527-3549. DOI:10.1007/s10661-012-2808-5

Kitanidis, P.K., 1997. Introduction to geostatistics. Cambridge University Press, Cambridge.

Kolovos, A., Christakos, G., Hristopulos, D.T., Serre, M.L., 2004. Methods for generating non-separable spatiotemporal covariance models with potential environmental applications. Adv. Water Resour. 27(8), 815-830.

Kritsotakis, M., 2010. Water resources management in Mesara valley of Crete (in Greek). PhD Thesis Thesis, Technical University of Crete, Chania, 700 pp.

Kumar, V., 2007. Optimal contour mapping of groundwater levels using universal kriging-a case study. Hydrolog. Sci. J. 52(5), 1038-1050.

Kyriakidis, P., Journel, A., 1999. Geostatistical Space-Time Models: A Review. Math. Geol. 31(6), 651-684.

Lee, S.J., Wentz, E.A., Gober, P., 2010. Space-time forecasting using soft geostatistics: A case study in forecasting municipal water demand for Phoenix, Arizona. Stoch. Env. Res. Risk A. 24(2), 283-295.

Lyon, S.W., Seibert, J., Lembo, A.J., Walter, M.T., Steenhuis, T.S., 2006. Geostatistical investigation into the temporal evolution of spatial structure in a shallow water table. Hydrol. Earth Syst. Sci. 10(1), 113-125. DOI:10.5194/hess-10-113-2006

ACCEPTED MANUSCRIPT

Ma, T.-S., Sophocleous, M., Yu, Y.-S., 1999. Geostatistical Applications in Ground-Water Modeling in South-Central Kansas. Journal of Hydrologic Engineering 4(1), 57-64. DOI:doi:10.1061/(ASCE)1084-0699(1999)4:1(57)

Olea, R.A., 1999. Geostatistics for engineers and earth scientists. Kluwer Academic Publishers, New York.

Pardo-Igúzquiza, E., Chica-Olmo, M., 2004. Estimation of gradients from sparse data by universal kriging. Water Resour. Res. 40(12). DOI:10.1029/2004wr003081

Pham, H., 2006. Springer Handbook of Engineering Statistics. Springer-Verlag, London.

Pilz, J., Spöck, G., 2008. Why do we need and how should we implement Bayesian kriging methods. Stoch. Env. Res. Risk A. 22(5), 621-632.

Porcu, E., Gregori, P., Mateu, J., 2006. Nonseparable stationary anisotropic space-time covariance functions. Stoch. Env. Res. Risk A. 21(2), 113-122.

Porcu, E., Mateu, J., Saura, F., 2008. New classes of covariance and spectral density functions for spatio-temporal modelling. Stoch. Env. Res. Risk A. 22(suppl.1), 65-79.

Raja, N.B., Aydin, O., Türkoğlu, N., Çiçek, I., 2017. Space-time kriging of precipitation variability in Turkey for the period 1976–2010. Theor. Appl. Climatol. 129(1), 293-304. DOI:10.1007/s00704-016-1788-8

Razavi, S., Tolson, B.A., Burn, D.H., 2012. Review of surrogate modeling in water resources. Water Resour. Res. 48(7). DOI:10.1029/2011wr011527

Rivest, M., Marcotte, D., Pasquier, P., 2008. Hydraulic head field estimation using kriging with an external drift: A way to consider conceptual model information. J. Hydrol. 361(3-4), 349-361.

Rodriguez-Iturbe, I., Mejia, M.J., 1974. The design of rainfall networks in time and space. Water Resour. Res. 10(4), 713–728.

Rouhani, S., 1986. Comparative study of ground-water mapping techniques. Ground Water 24(2), 207-216.

ACCEPTED MANUSCRIPT

Rouhani, S., Myers, D., 1990. Problems in space-time kriging of geohydrological data. Math. Geol. 22(5), 611-623.

Ruybal, C.J., Hogue, T.S., McCray, J.E., 2019. Evaluation of Groundwater Levels in the Arapahoe Aquifer Using Spatiotemporal Regression Kriging. Water Resour. Res. 55. DOI:10.1029/2018wr023437

Sakizadeh, M., Mohamed, M.M.A., Klammler, H., 2019. Trend Analysis and Spatial Prediction of Groundwater Levels Using Time Series Forecasting and a Novel Spatio-Temporal Method. Water Resour. Manag. DOI:10.1007/s11269-019-02208-9

Skøien, J.O., Blöschl, G., 2007. Spatiotemporal topological kriging of runoff time series. Water Resour. Res. 43(9).

Snepvangers, J.J.J.C., Heuvelink, G.B.M., Huisman, J.A., 2003. Soil water content interpolation using spatio-temporal kriging with external drift. Geoderma 112(3-4), 253-271.

Special water secretariat of Greece, 2015. Integrated Management Plans of the Greek Watersheds, Ministry of Environment & Energy, Athens.

Tadić, J.M., Qiu, X., Miller, S., Michalak, A.M., 2017. Spatio-temporal approach to moving window block kriging of satellite data v1.0. Geosci. Model Dev. 10(2), 709-720. DOI:10.5194/gmd-10-709-2017

Tapoglou, E., Karatzas, G.P., Trichakis, I.C., Varouchakis, E.A., 2014. A spatio-temporal hybrid neural network-Kriging model for groundwater level simulation. J. Hydrol. 519, Part D, 3193-3203. DOI:http://dx.doi.org/10.1016/j.jhydrol.2014.10.040

Theodoridou, P.G., Varouchakis, E.A., Karatzas, G.P., 2017. Spatial analysis of groundwater levels using Fuzzy Logic and geostatistical tools. J. Hydrol. 555, 242-252. DOI:https://doi.org/10.1016/j.jhydrol.2017.10.027

Theodossiou, N., Latinopoulos, P., 2006. Evaluation and optimisation of groundwater observation networks using the kriging methodology. Environ. Modell. Softw. 21(7), 991-1000.

Todd, D.K., 1959. Groundwater Hydrology. Wiley, New York, N.Y, 336 pp.

ACCEPTED MANUSCRIPT

Tonkin, M.J., Larson, S.P., 2002. Kriging water levels with a regional-linear and point-logarithmic drift. Ground Water 40(2), 185-193.

Varouchakis, E.A., 2016. Integrated Water Resources Analysis at Basin Scale: A Case Study in Greece. J. Irrig. Drain. E-ASCE 142(3), 05015012. DOI:10.1061/(ASCE)IR.1943-4774.0000966

Varouchakis, E.A., 2017. Spatiotemporal geostatistical modelling of groundwater level variations at basin scale: a case study at Crete's Mires Basin. Hydrology Research 49(4), 1131-1142. DOI:10.2166/nh.2017.146

Varouchakis, E.A., Hristopulos, D.T., 2013. Improvement of groundwater level prediction in sparsely gauged basins using physical laws and local geographic features as auxiliary variables. Adv. Water Resour. 52(2013), 34-49.

Varouchakis, E.A., Hristopulos, D.T., 2017. Comparison of spatiotemporal variogram functions based on a sparse dataset of groundwater level variations. Spatial Statistics. DOI:https://doi.org/10.1016/j.spasta.2017.07.003

Yang, D. et al., 2013. Solar irradiance forecasting using spatial-temporal covariance structures and time-forward kriging. Renewable Energy 60, 235-245. DOI:https://doi.org/10.1016/j.renene.2013.05.030

Zeng, Z. et al., 2014. A Regional Gap-Filling Method Based on Spatiotemporal Variogram Model of CO2 Columns. IEEE Trans. Geosci. Remote Sens. 52(6), 3594-3603. DOI:10.1109/TGRS.2013.2273807

Zhang, Y.K., Li, Z., 2005. Temporal scaling of hydraulic head fluctuations: Nonstationary spectral analyses and numerical simulations. Water Resour. Res. 41(7), 1-10.

Zhao, Y., Lu, W., Xiao, C., 2016. A Kriging surrogate model coupled in simulation–optimization approach for identifying release history of groundwater sources. J. Contam. Hydrol. 185-186, 51-60. DOI:https://doi.org/10.1016/j.jconhyd.2016.01.004

ACCEPTED MANUSCRIPT

Captions

Fig. 1 Location of the study area accompanied by topographic, hydrogeological and land use information; the distance metrics that connect the monitoring locations are presented

Fig. 2 Space-time variogram fitting of the product-sum model (left) and of the Spartan structure (right) to the experimental variogram; the variograms parameters are presented: $\sigma_z^2 =$ is the variance (sill), ξ_r, ξ_τ are spatial and temporal correlation lengths, η_1 is Spartan model shape coefficient, α is a relative weight of the time lag with respect to the spatial lag, c the nugget variance and k_1, k_2, k_3 coefficients of the product sum model.

Fig. 3 Aquifer level estimation (meters above sea level, masl) and predictions uncertainty at Mires basin: 2014-15 Wet Period mean CDF (middle), 5% (bottom) and 95% (top) levels of CDF (cumulative distribution function).

Fig. 4 Aquifer level estimation (meters above sea level, masl) and predictions uncertainty at Mires basin: 2014-15 Dry Period, mean CDF (middle), 5% (bottom) and 95% (top) levels of CDF (cumulative distribution function).

Fig. 5 East-West cross section of the study aquifer presenting hydrogeological and topographic information and the aquifer level distribution highlighting the higher and lower locations of estimations uncertainty (modified after (Kritsotakis, 2010))

Fig. 6 South-North cross section of the study aquifer presenting hydrogeological and topographic information and the aquifer level distribution highlighting the higher and lower locations of estimations uncertainty (modified after (Kritsotakis, 2010))

Fig. 7 Posterior distribution of the most important parameters of the Bayesian space-time geostatistical model; w is a weight parameter of the EWMA filter, ξ_r, ξ_τ are the spatial and temporal correlation lengths and η_1 is Spartan model shape coefficient

Fig. 8 Average spatial distribution of STRK standard deviation of residuals (uncertainty) in meters above sea level at Mires Basin

Figure 1

ACCEPTED MANUSCRIPT

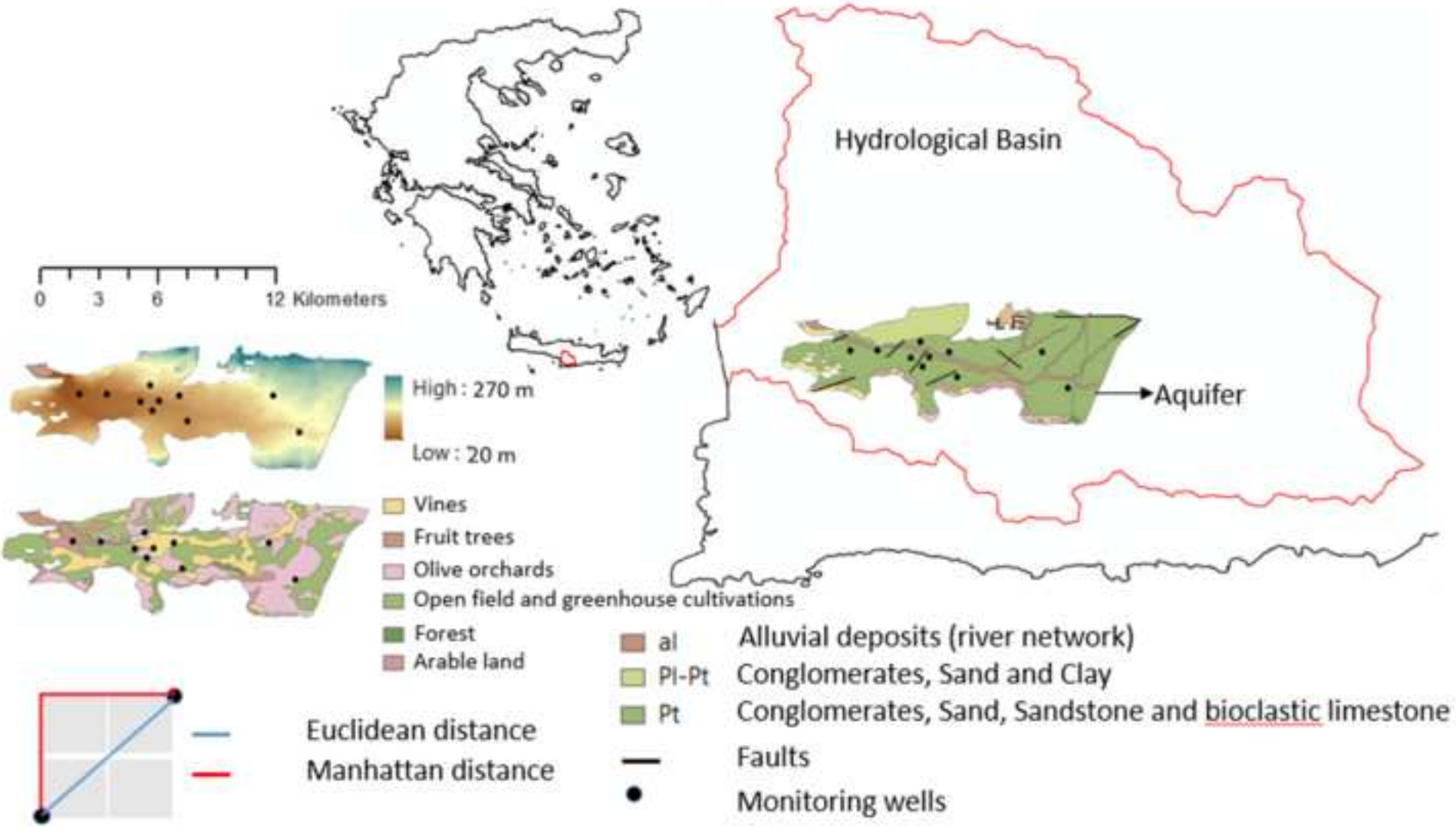

Figure 2

ACCEPTED MANUSCRIPT

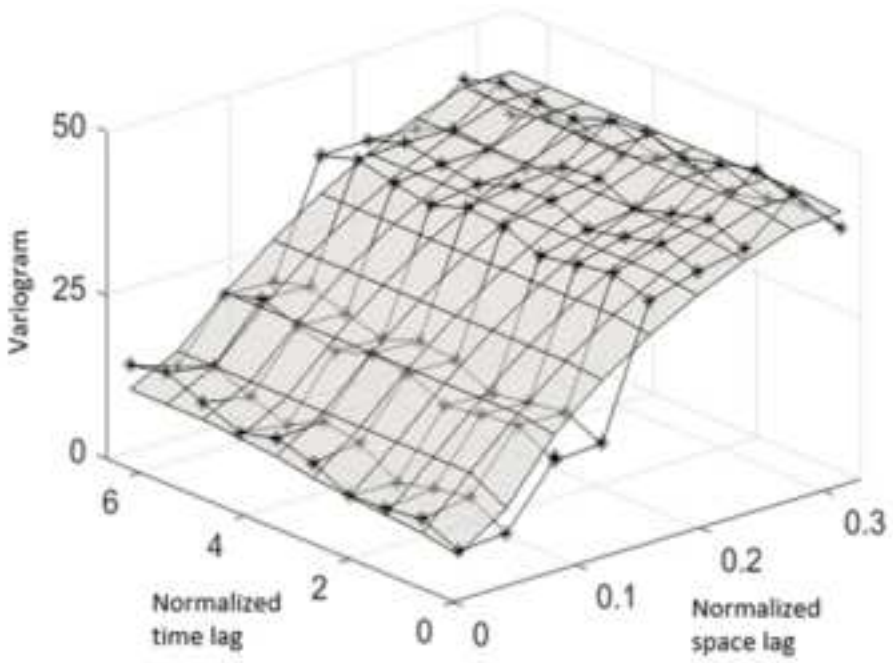

$\sigma_{\varepsilon_1}^2 = 41.96\,\mathrm{m}^2$, $\xi_s = 0.31$ (≈ 3.5 km), $\xi_t = 0.47$ (≈ 6 months), $\sigma_{\varepsilon_2}^2 = 44.36\,\mathrm{m}^2$

nugget variance $c = 5.28\ \mathrm{m}^2$ and $k_1 = 0.27$, $k_2 = 1.14$, $k_3 = 1.47$

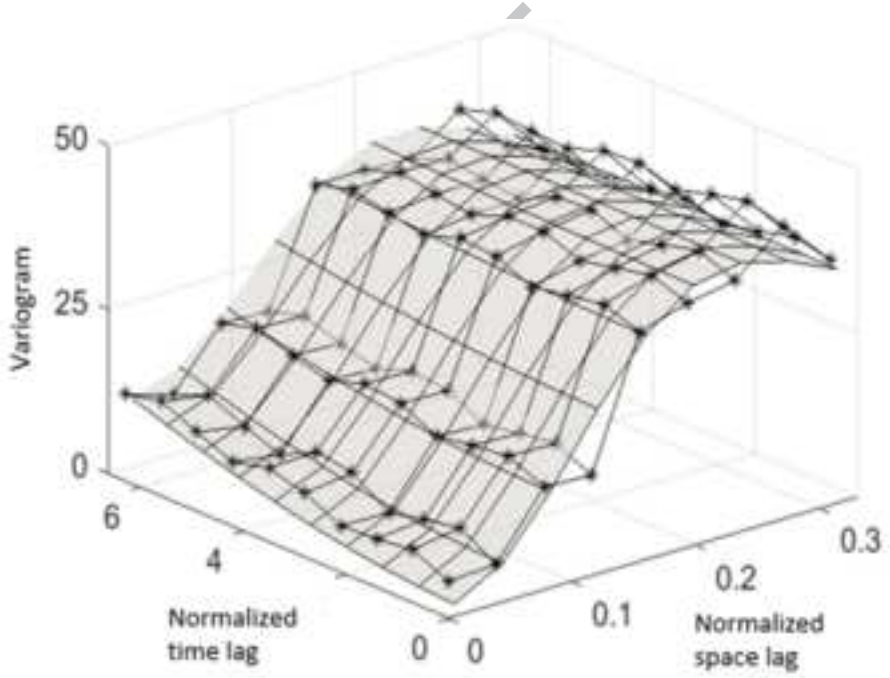

$\sigma_z^2 = 46.60\ \mathrm{m}^2$, $\xi_s = 0.27$ (≈ 3km), $\xi_t = 0.94$ (≈ 12 months)

$\eta_1 = 1.87$, $\alpha = 0.12$ and nugget variance $c = 3.83\ \mathrm{m}^2$

Figure 3

ACCEPTED MANUSCRIPT

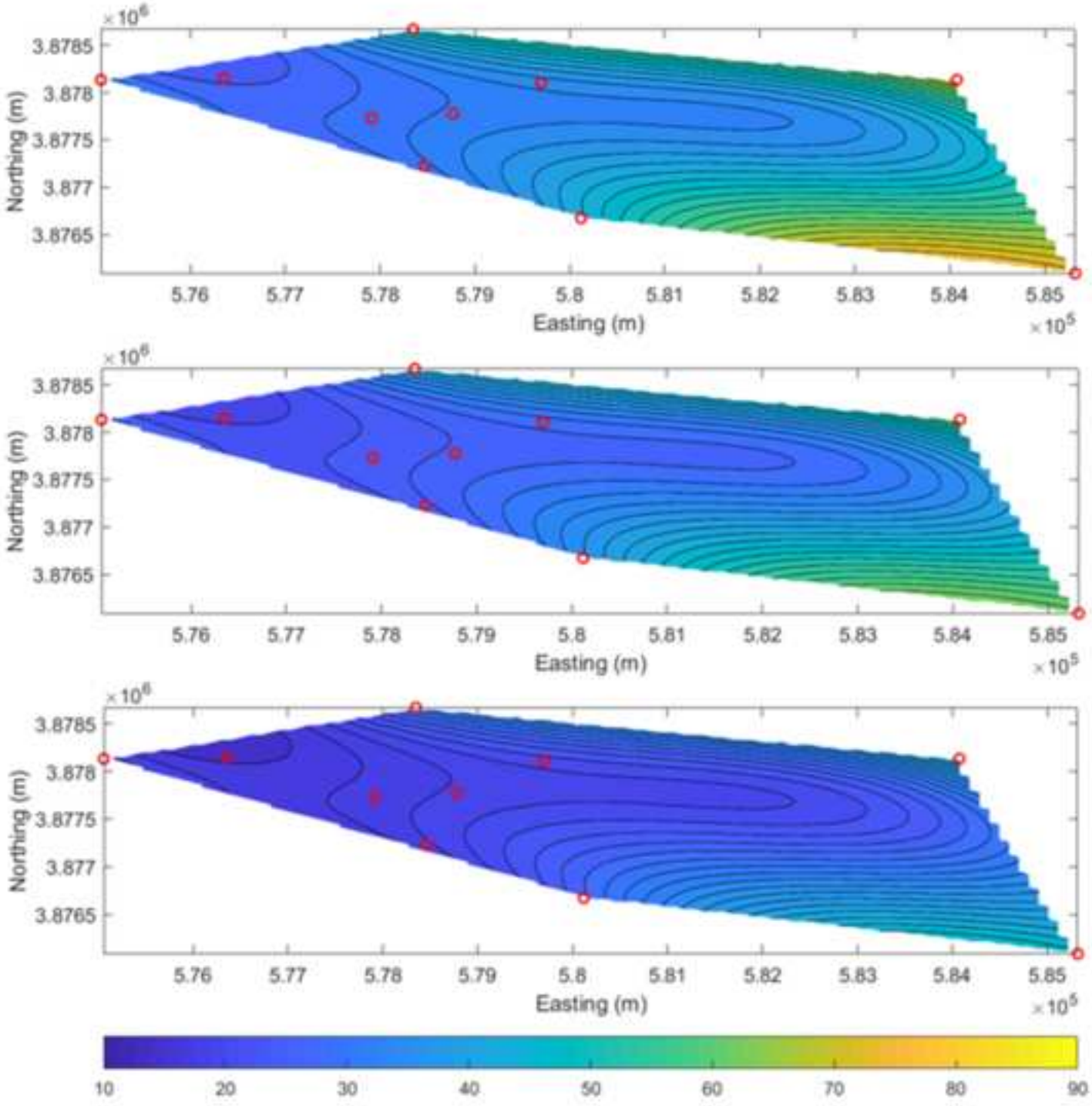

Figure 4

ACCEPTED MANUSCRIPT

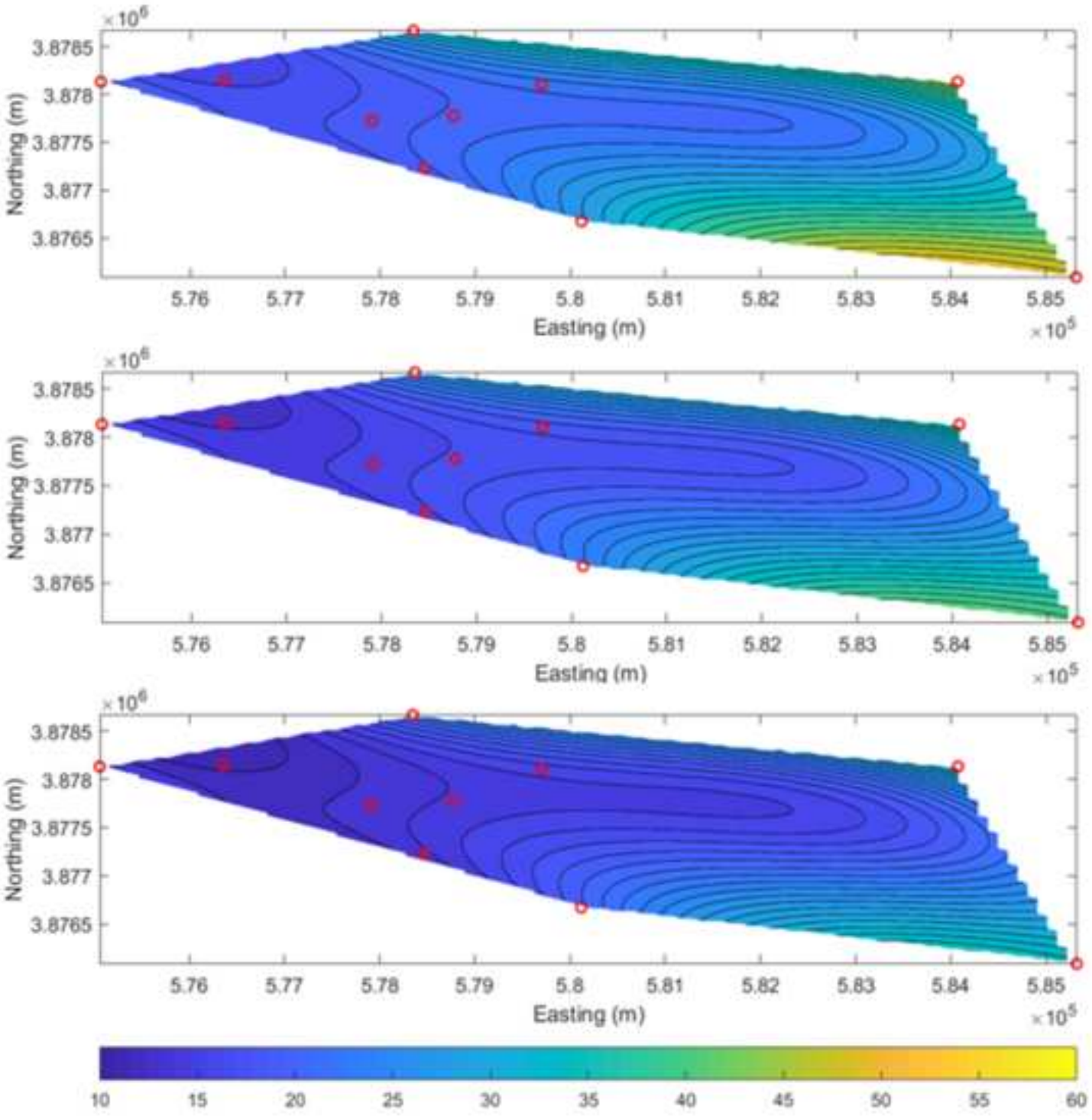

Figure 5

ACCEPTED MANUSCRIPT

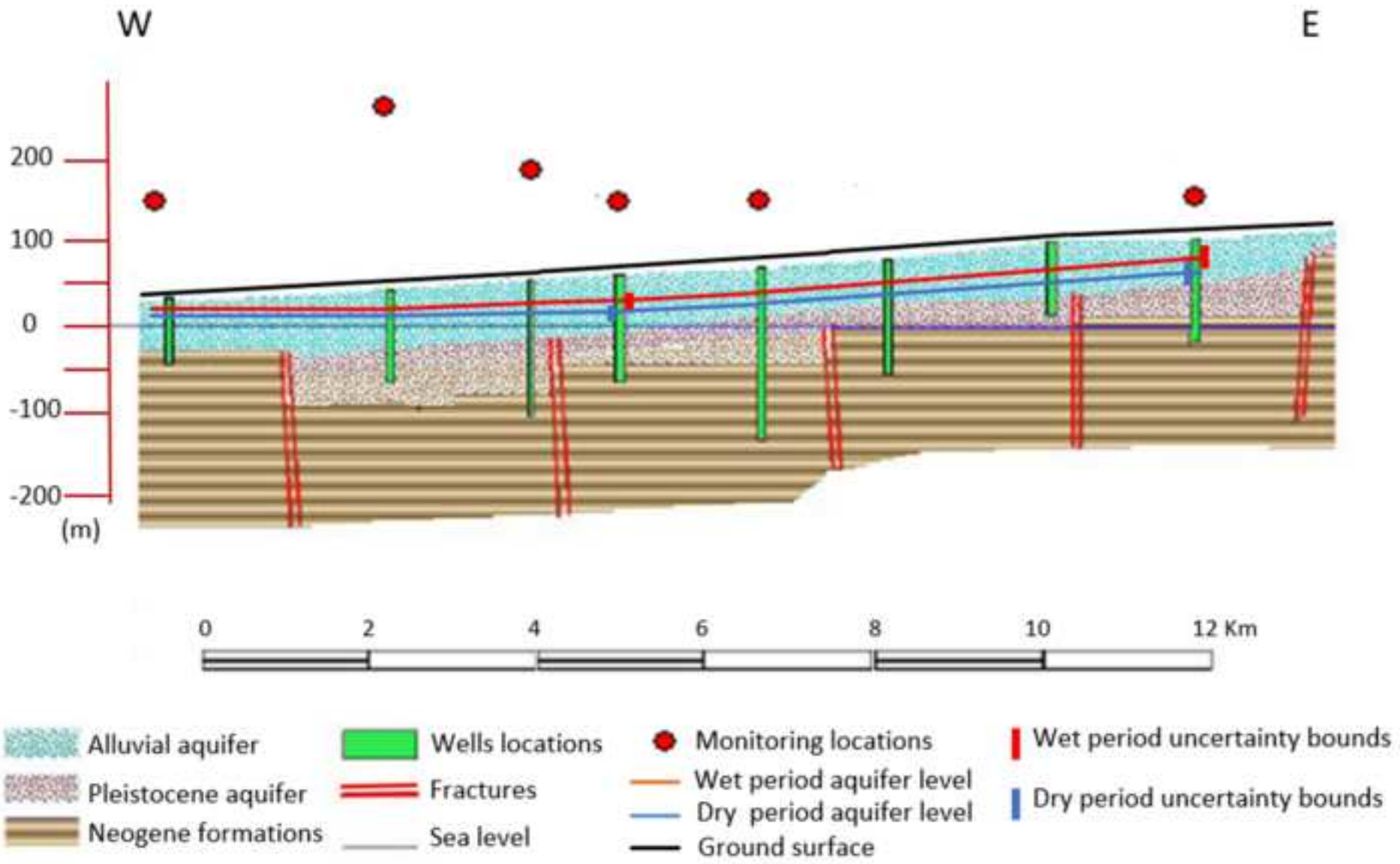

Figure 6

ACCEPTED MANUSCRIPT

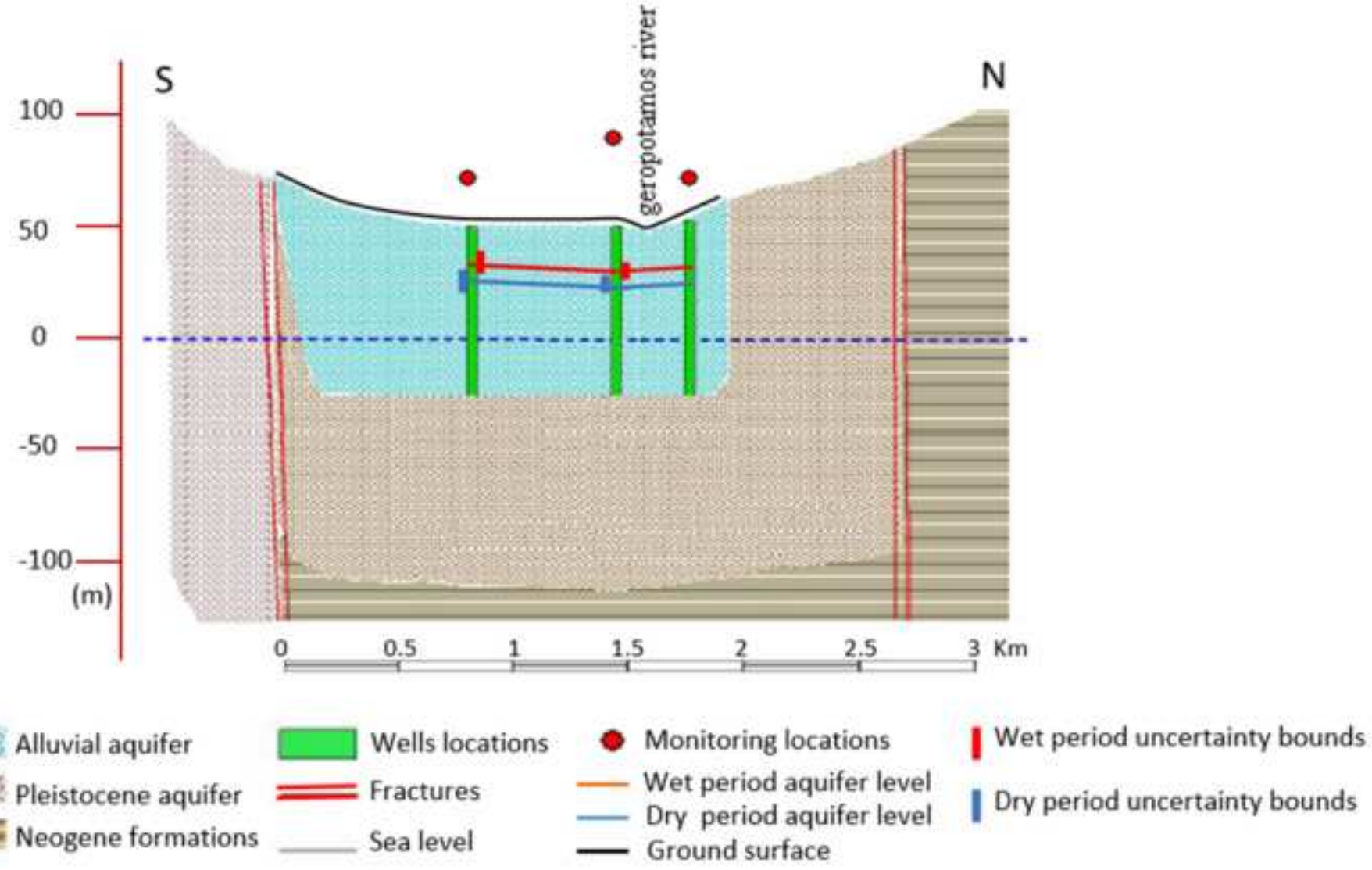

Figure 7

ACCEPTED MANUSCRIPT

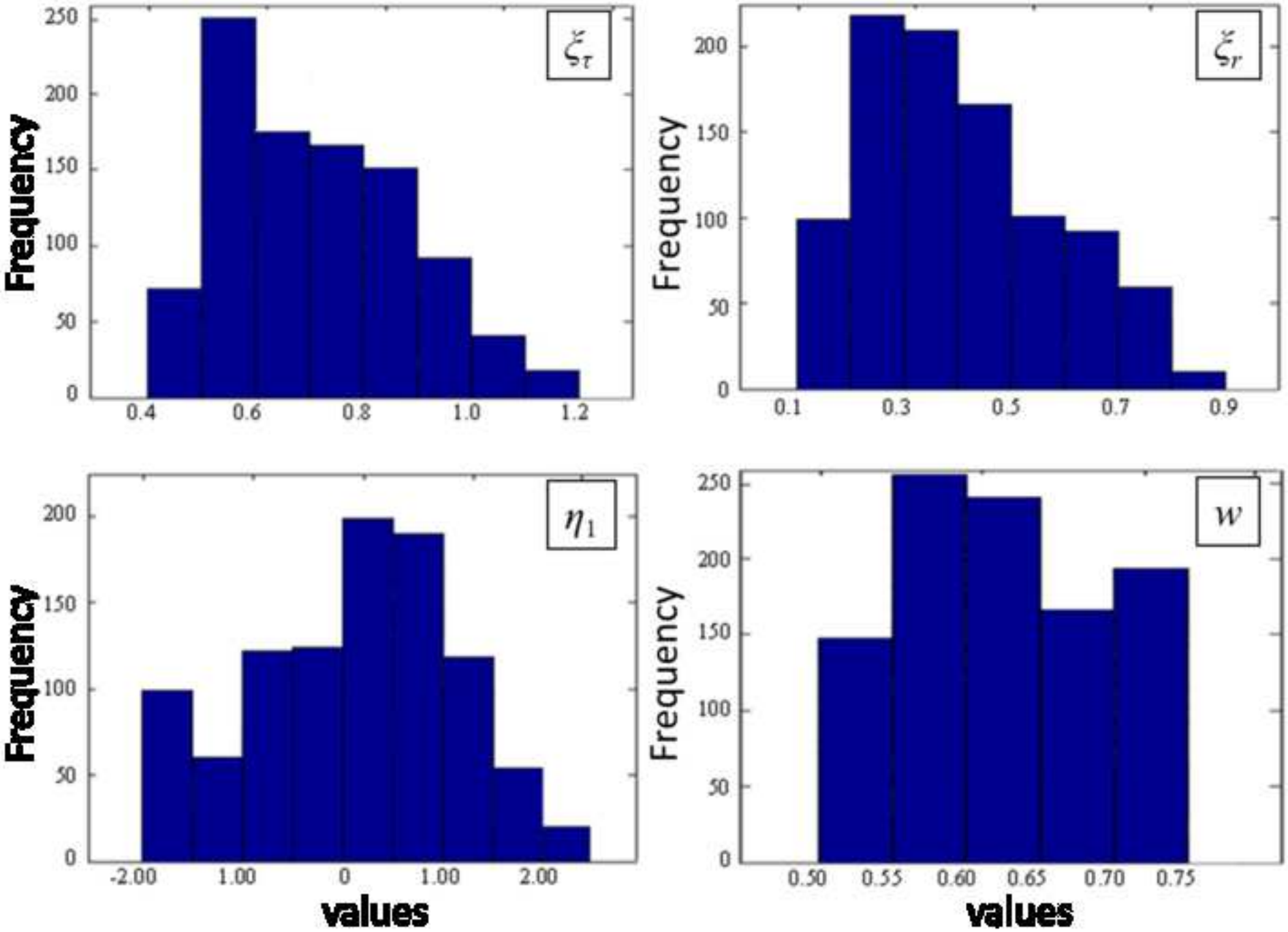

Figure 8

ACCEPTED MANUSCRIPT

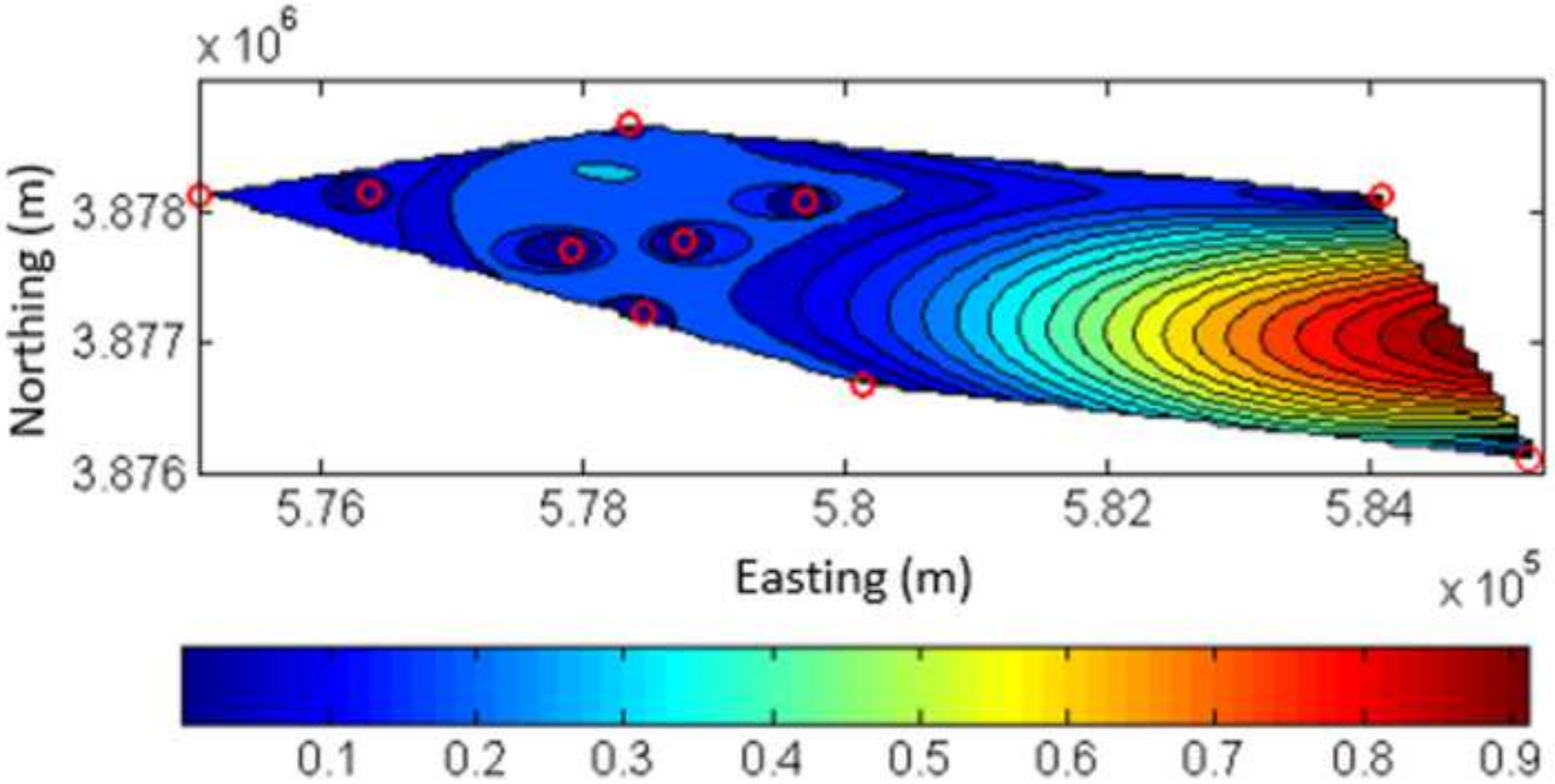

ACCEPTED MANUSCRIPT

Highlights

- *A new Spartan type space-time variogram efficiently determined data interdependence*
- *A product-sum variogram using hydraulic conductivity was successfully presented*
- *Space-time Bayesian kriging using bootstrap idea provided accurate estimations*
- *Bayesian bootstrap idea effectively determined estimations and parameters uncertainty*
- *A non-Euclidean distance metric improved the estimations accuracy*

ACCEPTED MANUSCRIPT